Time-resolved transillumination for medical diagnostics

Berg, R; Andersson-Engels, Stefan; Jarlman, O; Svanberg, Sune

Published in:
Time-Resolved Spectroscopy and Imaging of Tissues

DOI:
10.1117/12.44183

1991

Time-resolved Transillumination for Medical Diagnostics

R. Berg, S. Andersson-Engels, O. Jarlman* and S. Svanberg

Department of Physics, Lund Institute of Technology
P.O Box 118, S-221 00, Lund, Sweden. Telephone: (46) 46 107650

*Department of Diagnostic Radiology, Lund University Hospital
S-221 85, Lund, Sweden. Telephone: (46) 46 171000

ABSTRACT

We demonstrate a time-gated technique to reduce the effect of light scattering when transilluminating turbid media such as tissue. The concept is based on transillumination with picosecond laser pulses and time-resolved detection. By detecting only the photons with the shortest travelling time, and thus the least scattered photons, the contrast can be enhanced. Measurements on a tissue phantom as well as breast tissue *in vitro* are presented. It is demonstrated that differences in scattering properties may be more pronounced than differences in absorption properties when demarcating tumor from normal tissue.

1. INTRODUCTION

Visible light transillumination of tissue is a diagnostic modality based on the characteristic absorption of light in malignant tumors due to the surrounding neovascularization.[1-6]
In optical transillumination, wavelengths with low absorption have to be used, i.e. red or near-infrared light. The main problem is that in this wavelength region the dominating attenuation effect is not absorption but scattering. The scattering coefficient is of the order of 100 cm^{-1}, while the absorption coefficient is of the order of 1 cm^{-1}.[7-9] The large scattering coefficient induces a pronounced multiple scattering in the tissue. The effect causes a decreased contrast when tissue transillumination is performed. We demonstrate a time-gating technique to reduce the effect of light scattering.[10-11]
The time-gating technique is based on the concept that light which leaves the transilluminated tissue first has traveled a shorter and straighter path in the tissue than light exiting later[12-13]. This early light thus contains more information about the spatial localization of different optical properties.
Recently several other approaches have been presented. Spears et al. have used a technique called chrono-coherent imaging in which the transmitted light is detected on a hologram by means of a reference beam acting as an ultrafast light shutter (Light in flight)[14]. Toida et al. have used a technique based on heterodyne detection.[15]

2. THEORETICAL MODELS

Different models can be used to simulate the photon propagation in tissue. One way is to use Monte Carlo simulations. In this approach the path of a single photon in the tissue is tracked. The tissue is characterized by the scattering coefficient

 0-8194-0521-3/91/$4.00

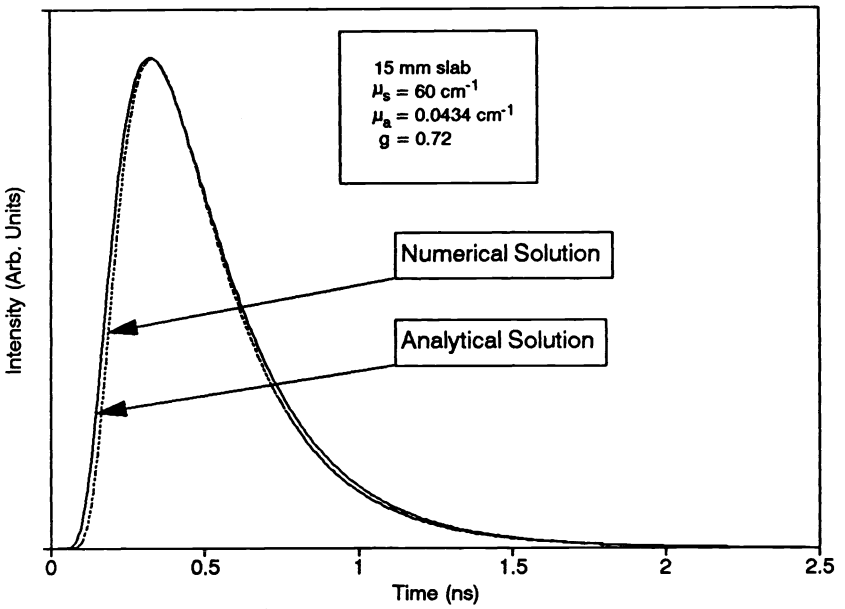

Fig. 1. *Comparison between analytical and numerical solution of the diffusion equation when modeling tissue transillumination.*

(μs), the absorption coefficient (μa) and the mean cosine of the scattering angle (g), which is a way of expressing the anisotropic scattering of the photons. By tracking a large number of photons it is possible to simulate the behavior of the light in tissue.
Another model is based on the diffusion equation:

$$(1/c)\,\frac{\partial\Phi(\mathbf{r},t)}{\partial t} - D\nabla^2\Phi(\mathbf{r},t) + \mu a\Phi(\mathbf{r},t) = S(\mathbf{r},t) \qquad (1)$$

where $\Phi(\mathbf{r},t)$ is the diffuse photon fluence rate, c is the speed of light in the tissue, D is the diffusion coefficient ($D=(3(\mu a+(1-g)\mu s))^{-1}$) and $S(\mathbf{r},t)$ is the photon source. The equation can be solved numerically by using a computer and thus the light propagation can be calculated for different kinds of tissue. Patterson et al. have solved the equation analytically for transillumination of a homogeneous tissue slab[16]. In Fig. 1 we show a comparison between the analytical solution (solid curve) and a numerically computed solution (dashed curve) when transilluminating a 15 mm thick tissue slab with $\mu s = 60$ cm^{-1}, $\mu a = 0.0434$ cm^{-1} and $g=0.72$. In the numerical model we have used a 10×25×25 matrix. Although the numerical model is rather coarse the agreement between the two models is good. To verify the computer models and also simulate different kinds of tissue, phantoms with given optical properties can be made by mixing liquids with known scattering coefficient (Intralipid) and absorption coefficient (ink). Fig. 2 shows the result when transilluminating a 30 mm thick tissue phantom of Intralipid and ink (solid curve). The optical properties of the mixture are estimated to be $\mu s = 60$ cm^{-1} and $\mu a = 0.15$. A comparison with the analytical solution (dashed curve) gives $\mu s = 60$ cm^{-1}, $\mu a = 0.12$ cm^{-1} with $g=0.8$.

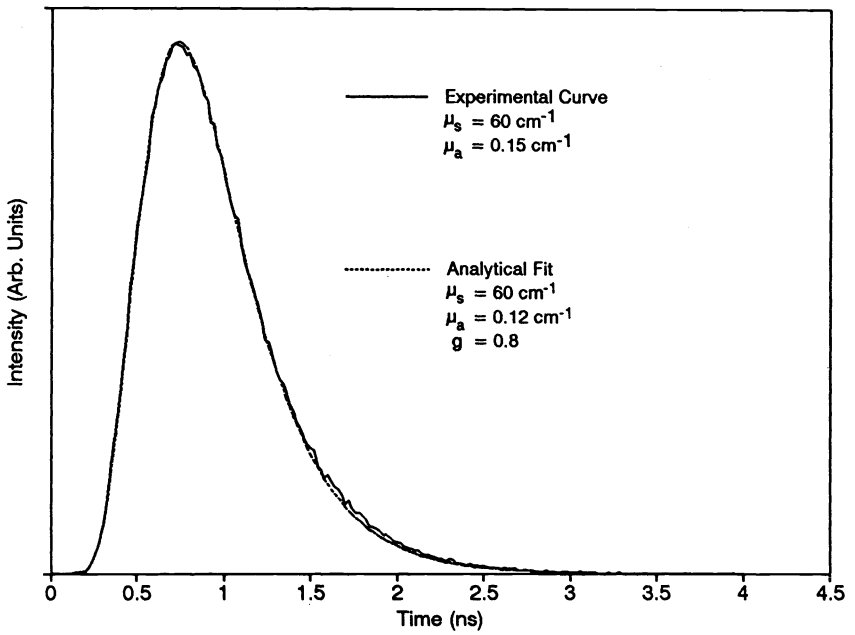

Fig. 2. *Experimental curve of detected light intensity when transilluminating a liquid tissue phantom and a fit to that curve using an analytical model. The fitting parameters agree well with the experimentally given.*

3. EXPERIMENTAL SET-UP

The experimental set-up used in our studies of photon migration in tissue is shown in Fig. 3. The light source was a mode-locked Coherent CR-12 Ar-ion laser pumping a Coherent CR-599 dye laser equipped with a cavity dumper. The pulses from the dye laser were measured to be 6 psec wide by using an autocorrelator. The laser pulses irradiated the object, and the light was detected on the opposite side. The detector assembly consists of a small aperture and a lens that focuses the light onto an optical fiber. Delayed coincidence techniques were used to achieve time-resolved detection. The detector fiber is connected to a photon-counting microchannel plate (Hamamatsu R2566-07), and the signal is fed through a fast amplifier and a constant fraction discriminator (CFD) to a time-to-amplitude converter. This signal is the start signal for the time-to-amplitude converter. The stop signal comes from a diode triggering on the incident pulse. The trigger pulse is also fed through a fast amplifier and a CFD. The output signal from the time-to-amplitude converter is fed to a multichannel analyzer in which a histogram of arrival time for the photons is formed, i.e. a temporal dispersion curve. The curves can be transferred to a computer (PC) for evaluation. The impulse response function for the system is approximately 50 ps (FWHM). A small fraction of the incident light is brought to the detector directly to create a small peak in front of every curve. This peak is thus a reference in time and enables comparison between different detected curves.
The transilluminated sample can be translated across the beam-detector axis and scanning can thus be performed.

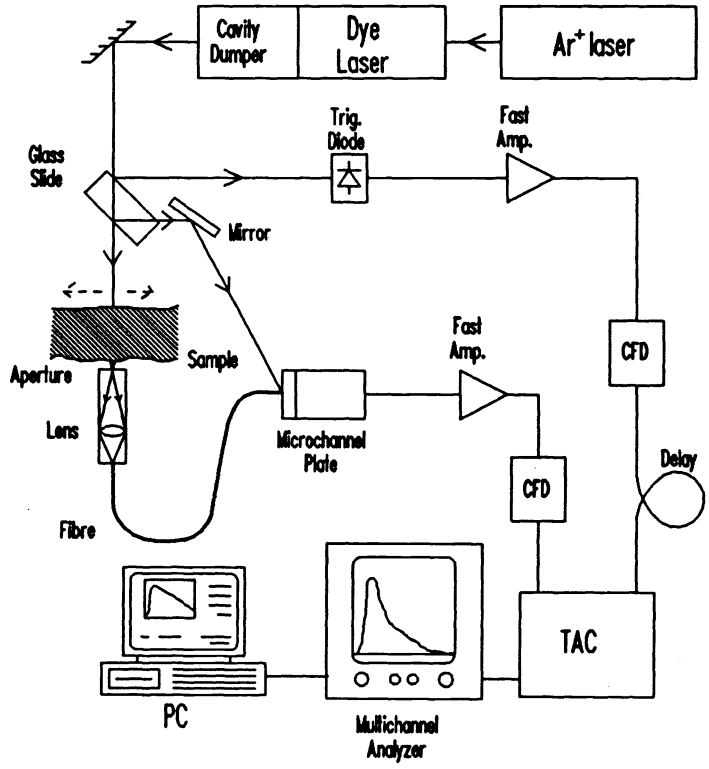

Fig. 3. *Experimental set-up used in the study of time-resolved migration of photons in tissue.*

4. RESULTS

4.1 Breast tissue

Fig. 4 shows a scan through a 16 mm thick slab of female breast *in vitro* with a malignant tumor. The diameter of the tumor was approximately 18 mm and it was an invasive ductal carcinoma. The laser wavelength in this case was 640 nm. A temporal dispersion curve was sampled for every 2 mm for 60 sec. The dashed curve shows the total amount of light received at every point (Time Integrated) and the solid curve shows the light received during the first 120 psec of every dispersion curve (Time Gated). The time gate window starts when the first light is detected (above noise level). The window is fixed in time to the previously mentioned reference peak and thus the window is kept constant when scanning over the sample. This presumes that the sample thickness is constant and that the refractive index does not change considerably over the sample. As can be seen there is a distinct demarcation of the tumor when the time gated technique is used. In this case the amount of early light increases through the tumor while the total amount of light remains almost constant. Fig. 5 shows the temporal dispersion curves received on the tumor and on both sides of the tumor. The curves are autoscaled. As can be seen there is a large difference in the shape of the curves and it can also be seen that the curve obtained on the tumor possesses a lot more early light. The reason for this can be found in the difference in scattering coefficient. By doing a least-square fit to the analytical solution to equation (1) the optical properties of the tissue can be estimated. It gives $\mu_s = 68$ cm^{-1} and $\mu_a = 0.22$ cm^{-1} for the tumor and $\mu_s = 98$ cm^{-1} and $\mu_a = 0.21$ cm^{-1} for the healthy tissue just next to the tumor. This is calculated with

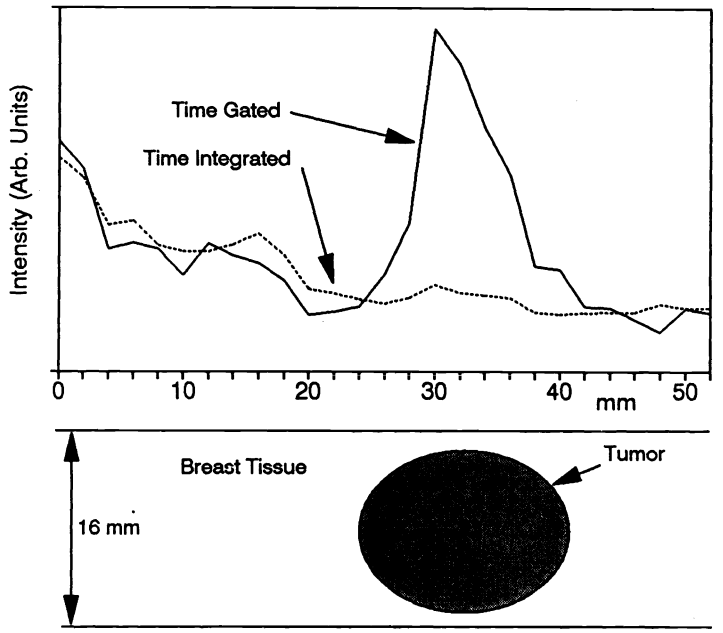

Fig. 4. *Detected light intensity when scanning* in vitro *across a 16 mm thick slab of female breast with a malignant tumor.*

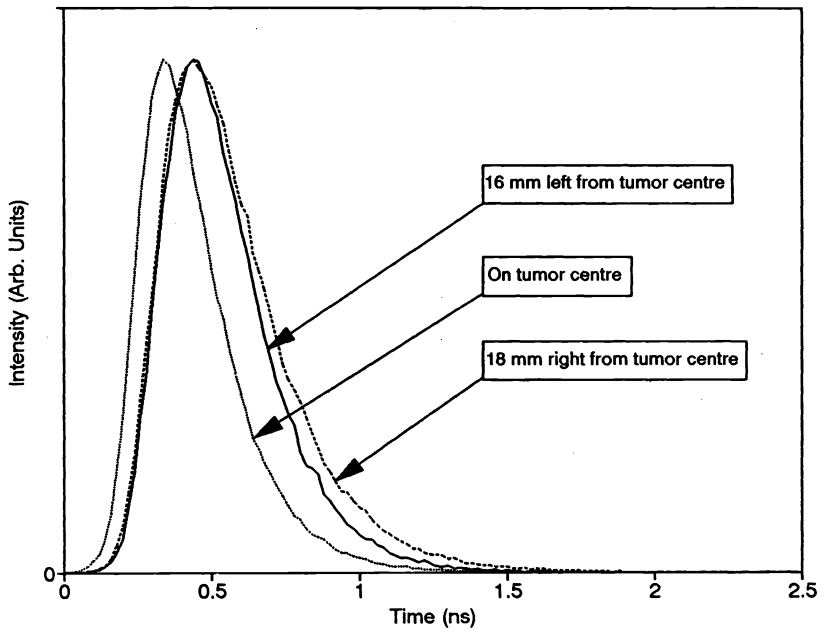

Fig. 5. *Temporal dispersion curves obtained through tumor tissue and on both sides of the tumor.*

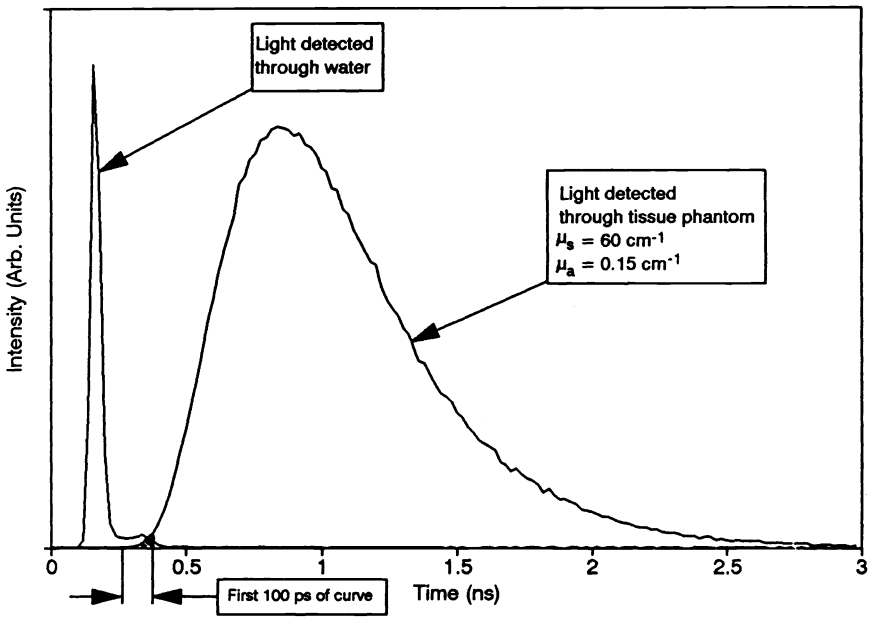

Fig. 6. *Light detected through a 30 mm thick tissue phantom and through 30 mm of water. A time gate window of 100 psec is indicated on the curve detected through the phantom.*

g=0.8. The over-all slope of the curves in Fig. 4 is due to a varying absorption coefficient over the sample. The large scattering coefficient means that the detected early light is not unscattered light. The amount of unscattered light should be too small to detect. Fig. 6 shows the location in time of a time gate window of 100 psec on a dispersion curve detected through a 30 mm thick tissue phantom. The figure also shows the light detected when the phantom is substituted with water. The start of the time gate window is where the detected light rises above noise level and thus it can be seen in the figure that no direct unscattered light can be detected through the tissue phantom.

4.2 Tissue phantom

Fig. 7A shows a scan through a tissue phantom consisting of a 30 mm cuvette filled with Intralipid and ink. The optical constants are estimated to $\mu s=50$ cm^{-1} and $\mu a=0.075$ cm^{-1}. A 10 mm diameter glass tube is put in the middle of the cuvette and filled with the same liquid. The dashed curve shows the total amount of light received and the solid curve the light received during the first 120 psec of every curve. As can be seen the glass tube can be detected when the time gated technique is used but it is hardly noticeable in the time integrated light. Fig. 7B shows the same type of scan but here the glass tube is filled with another liquid with $\mu s=40$ cm^{-1} and $\mu a=0.30$ cm^{-1}. As can be seen the tube can now be detected with the time integrated light and the intensity decreases when scanning over the tube due to the increased absorption coefficient. The time gated light intensity increases now even more and the demarcation of the tube is 50 % stronger than before. This is due to the decreased scattering coefficient of the liquid in the glass tube.

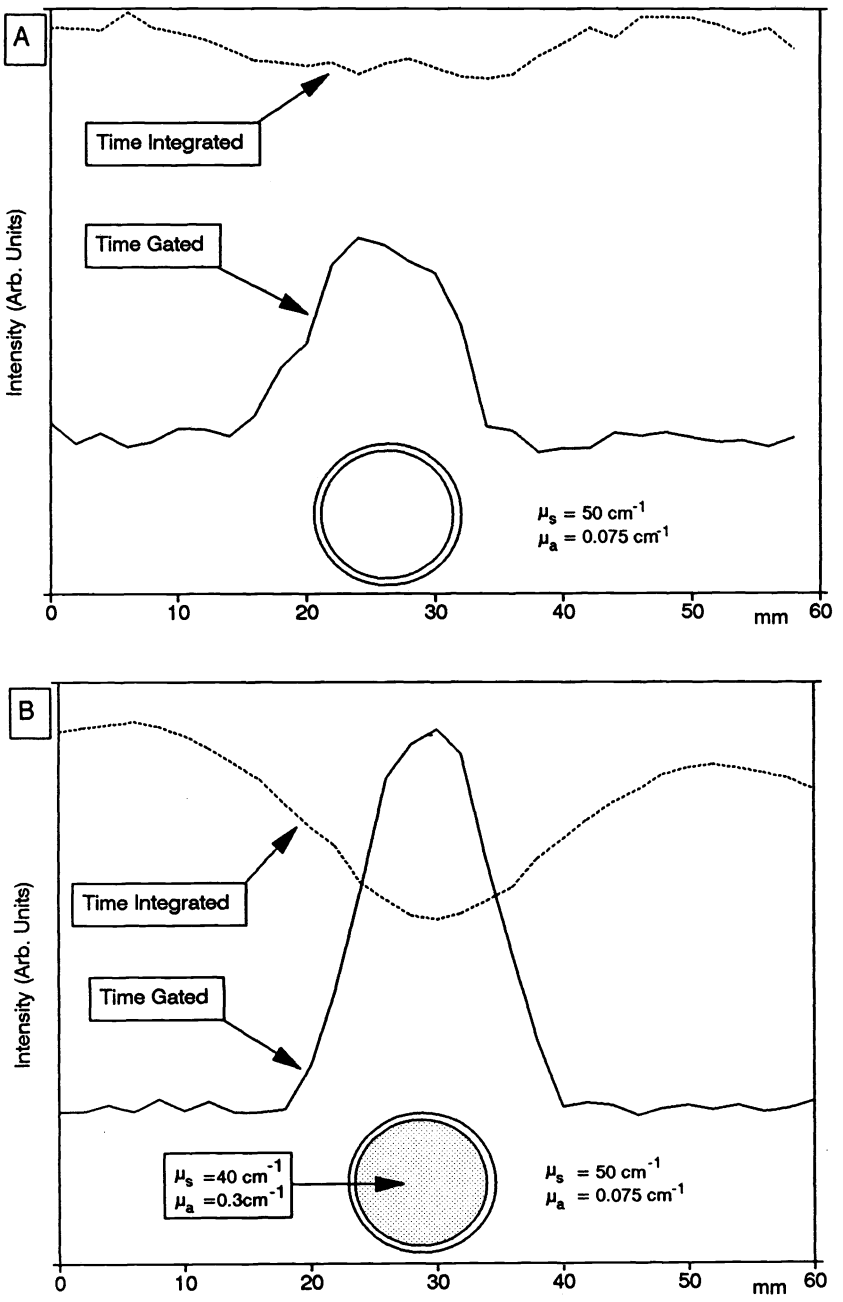

Fig. 7. *Detected light intensity when scanning over a tissue phantom with a glass tube inside it. The dashed curves show the total amount of light and the solid curves show the light detected during the first 120 psec. A: the tube containing same liquid as the rest of the phantom. B: the tube containing a different liquid.*

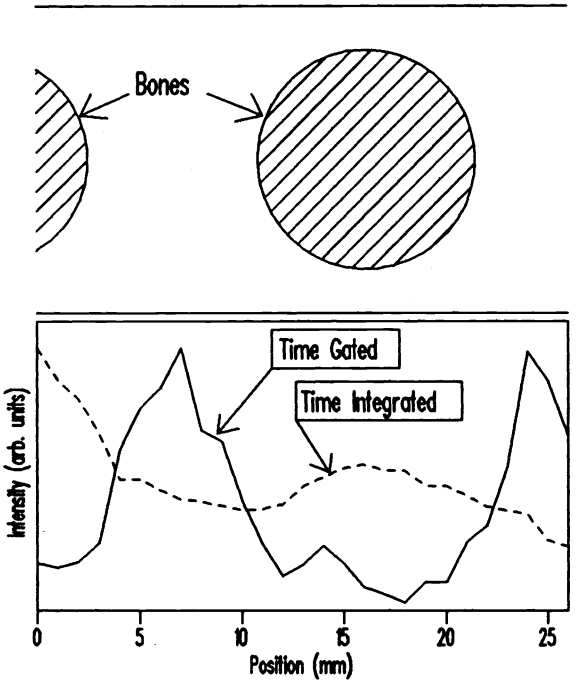

Fig. 8. *Detected light intensity when scanning across a hand in vivo. The solid curve correspond to the light detected during the first 80 psec. The dashed curve is the total detected light.*

4.3 Human hand

Fig. 8 shows a similar scan across a human hand *in vivo*. The scan was performed approximately 10 mm below the knuckle of the middle finger. The solid curve corresponds to the light intensity detected during the first 80 psec, and the dashed curve shows the total amount of light detected. As can be seen there is a significant demarcation of the bones. It should be noticed that the two curves are out of phase. The explanation to this could be that the scattering coefficient is larger and the absorption coefficient is smaller in the bones compared with the surrounding tissue.

5. DISCUSSION

Traditional diaphanography is based on the concept that the tumors have a higher absorption than the surrounding healthy tissue. Our experiments show that this is not always the case. Our results show that the difference in scattering coefficient can be the dominating optical property that differ between tumor and healthy tissue. By using the time gated technique and detecting only the early light the demarcation of the tumor can be strongly enhanced.

6. ACKNOWLEDGEMENTS

This work was supported by the Swedish Board for Technical Developments.

7. REFERENCES

1. B. Ohlsson, J. Gundersen and D.-M. Nilsson, "Diaphanography: A method for evaluation of the female breast," *World J. Surg.* **4**, pp. 701-705 (1980).

2. D. J. Watmough, "Transillumination of breast tissue: Factors governing optimal imaging of lesions," *Radiology* **147**, pp. 89-92 (1983).

3. B. Drexler, J. L. Davis and G. Schofield, "Diaphanography in the diagnosis of breast cancer," *Radiology* **157**, pp. 41-44 (1985).

4. S. Ertefai and A. E. Profio, "Spectral transmittance and contrast in breast diaphanography," *Med. Phys.* **12**, pp. 393-400 (1985).

5. G. A. Navarro and A. E. Profio, "Contrast in diaphanography of the breast," *Med. Phys.* **15**, pp. 181-187 (1988).

6. A. E. Profio, G. A. Navarro and O. W. Sartorius, "Scientific basis of breast diaphanography," *Med. Phys.* **16**, pp. 60-65 (1989).

7. B. C. Wilson, M. S. Patterson, S. T. Flock and D. R. Wyman, "Tissue Optical Properties in Relation to Light Propagation Models and in Vivo Dosimetry," in *Photon Migration in Tissue*, B. Chance, ed. (Plenum, New York, 1989).

8. D. T. Delpy, M. Cope, P. van der Zee, S. Arridge, S. Wray and J. Wyatt, "Estimation of optical pathlength through tissue from direct time of flight measurement," *Phys. Med. Biol.* **33**, pp. 1433-1442 (1988).

9. P. P. Ho, P. Baldeck, K. S. Wong, K. M. Yoo, D. Lee and R. R. Alfano, "Time dynamics of photon migration in semiopaque random media," *Appl. Opt.* **28**, pp. 2304-2310 (1989).

10. S. Andersson-Engels, R. Berg, J. Johansson, K. Svanberg and S. Svanberg, "Medical application of laser spectroscopy," in *Laser Spectroscopy IX*, M. Feld, ed., pp. 500-504 (Academic Press, New York, 1989).

11. S. Andersson-Engels, R. Berg, S. Svanberg and O. Jarlman, "Time-resolved transillumination for medical diagnostics," *Opt. Lett.* **15**, pp. 1179-1181 (1990).

12. J. M. Maarek, G. Jarry, J. Crowe, Bui M.-H. and D. Laurent, "Simulation of laser tomoscopy in a heterogeneous biological medium," *Med. & Biol. Eng. & Comput.* **24**, pp. 407-414 (1986).

13. J. C. Hebden and R. A. Kruger, "Transillumination imaging performance: A time-of-flight imaging system," *Med. Phys.* **17**, pp. 351-356 (1990).

14. K. G. Spears, J. Serafin, N. H. Abramson, X. Zhu and H. Bjelkhagen, "Chrono-coherent imaging for medicine," *IEEE Trans. Biomed. Eng.* **36**, pp. 1210-1221 (1989).

15. M. Toida, T. Ichimura and H. Inaba, "Approach to optical computer tomography for highly scattering biological subjects using an optical heterodyne technique," in *Conference on Lasers and Electro-Optics*, 1990 Technical Digest Series **7**, pp. 548-550 (Optical Society of America, Washington, DC, 1990).

16. M. S. Patterson, B. Chance and B. C. Wilson, "Time resolved reflectance and transmittance for the non-invasive measurement of optical properties," *Appl. Opt.* **28**, pp. 2331-2336 (1989).